CFD Simulation of Multi-Dimensional Effects in an Inertance Tube Pulse Tube Refrigerator

J.S. Cha[1], S.M. Ghiaasiaan[1], P.V. Desai[1], J.P. Harvey[2], and C.S. Kirkconnell[2]

[1]G.W. Woodruff School of Mechanical Engineering
Georgia Institute of Technology, Atlanta, GA 30332, U.S.A.

[2]Raytheon Space and Airborne Systems
El Segundo, CA 90245-0902, U.S.A.

ABSTRACT

Two entire Inertance Tube Pulse Tube Refrigerator (ITPTR) systems operating under a variety of thermal boundary conditions were modeled using a Computational Fluid Dynamics (CFD) code. Each simulated ITPTRs included a compressor, an after cooler, a regenerator, a pulse tube, cold and hot heat exchangers, an inertance tube, and a reservoir. The simulations represented fully coupled systems operating in steady-periodic mode. The objectives were to ascertain the suitability of CFD methods for ITPTRs and to examine the extent of multi-dimensional flow effects in various ITPTR components. The results confirmed that CFD simulations are capable of elucidating complex periodic processes in ITPTRs. The results also showed that a one-dimensional modeling is appropriate only when all the components in the system have large length-to-diameter (L/D) ratios. Significant multi-dimensional flow effects occur at the vicinity of component-to-component junctions, and secondary-flow recirculation patterns develop when one or more components have small L/D ratios.

INTRODUCTION

The design of Pulse Tube Refrigerator (PTR) systems has advanced incessantly since the invention of basic PTR[1], leading to improvements in their performance and lower achievable refrigeration temperatures. The major design variations introduced thus far include the Orifice Pulse Tube Refrigerator (OPTR)[2], double inlet OPTR[3], the modified OPTR[4], the multi-pass OPTR[5], and most recently the Inertance Tube Pulse Tube Refrigerator (ITPTR).[6] The exact nature of the physical phenomena underlying the operation of PTRs is not well-understood, however.[7,8] A fundamental difficulty in all PTRs is that their working fluid compression and expansion processes are not well-defined, and poorly-understood thermal relaxation and phase-lag phenomena dominate their operation. Crucial among these is the phase angle between pressure and mass flow. This phase angle is influenced by the wave resonance phenomena in BPTRs, and is adjusted by orifices and/or valves in various OPTR designs. In an ITPTR, the orifice valve of the simple OPTR is replaced by a long and slender (Inertance) tube that, with proper design, can cause an optimal phase lag between pressure and mass flow rate in the pulse tube.

Cryocoolers 13, edited by R. G. Ross, Jr.
Springer Science+Business Media, Inc., New York, 2004

Computational models have recently been developed for the simulation of the regenerator, or the entire PTR.[10-12] The Sage computer package [9] models an entire PTR assuming 1-D flow, and can optimize a system against a user-selected geometric parameter. The numerical model used by Ju et al.[10] is also 1-D and appears to simulate an entire PTR system. Simulation of a complete PTR system using CFD software packages has also been recently published.

Hozumi et al.[11] performed axi-symmetric and 3-D simulations of BPTRs and OPTRs, with an interest in the effects of gravity and orientation on system performance. Flake and Razani[12] conducted an axi-symmetric analysis of a BPTR and an OPTR, using the Fluent®[13] commercial CFD package, and indicated that the occurrence of recirculation patterns and streaming effects in the simulated pulse tube.

In this paper, we report on CFD simulations addressing the steady-periodic operation of two ITPTR systems. The objectives were to assess the feasibility of CFD simulation of ITPTRs, and to examine the extent and significance of multi-dimensional flow effects in these systems.

SIMULATED SYSTEMS

Two ITPTR systems referred to as MOD1 and MOD2 hereafter, were simulated, using the Fluent[13] code. A schematic of the ITPTR system is shown in Figure 1, and the geometric dimensions of all the components are listed in Table 1. The system designated as MOD1 is in fact identical to the experimental test apparatus of Kirkconnell et al.[14,15] and Harvey et al.[16], with the exception that MOD1 includes an inertance tube (IT) instead of an orifice. The MOD2 system is similar to MOD1, except that the regenerator, pulse tube, and inertance tube components of MOD2 have different geometric dimensions than MOD1.

Three different operational modes were simulated for MOD1 and MOD2 each, as summarized in Table 2. The three cases for each system address operation with an adiabatic cold end heat exchanger (CHX) (i.e., zero cooling load), a specified CHX cooling load, and a known CHX surface temperature. The boundary conditions depicted in Table 2 were the only parameters that were provided to the forthcoming CFD simulations. The entries that are shown in bold characters, furthermore, are calculated results from simulations. All other system boundaries were assumed to be adiabatic.

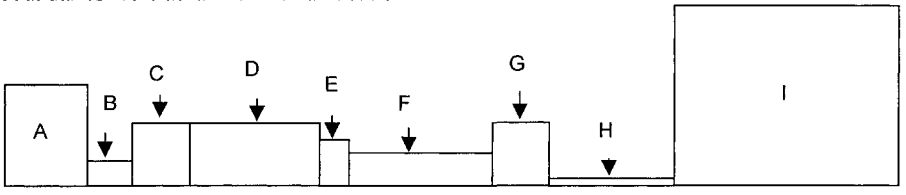

Figure 1. The Simulated ITPTR System.

Table 1. Dimensions of the Simulated Systems

	MOD1		MOD2	
Components	Radius (m)	Length (m)	Radius (m)	Length (m)
A (Compressor)	9.54E-03	7.50E-03	9.54E-03	7.50E-03
B (Transfer Line)	1.55E-03	1.01E-01	1.55E-03	1.01E-01
C (WHX1)	4.00E-03	2.00E-02	4.00E-03	2.00E-02
D (Regenerator)	4.00E-03	5.80E-02	1.00E-02	2.50E-02
E (CHX)	3.00E-03	5.70E-03	3.00E-03	5.70E-03
F (Pulse Tube)	2.50E-03	6.00E-02	7.50E-03	3.00E-02
G (WHX2)	4.00E-03	1.00E-02	4.00E-03	1.00E-02
H (Inert. Tube)	4.25E-04	6.84E-01	5.96E-04	1.07E+00
I (Surge Volume)	1.30E-02	1.30E-01	1.30E-02	1.30E-01

Table 2. Boundary Conditions for the Simulations

	MOD1			MOD2		
Components	Case 1	Case 2	Case 3	Case 4	Case 5	Case 6
WHX1 Wall Temperature (K)	293	293	293	293	293	293
CHX Wall Conditions	Adiabatic	1W load	150 K	Adiabatic	1 W load	282 K
WHX2 Wall Temperature (K)	293	293	293	293	293	293
CHX Load (W)	0	1	**6.39***	0	1	**2.57***
CHX Surface Temperature (K)	**87***	**100***	150	**278***	**280***	282

* These values were obtained from simulations.

CFD MODELS

The commercial CFD code Fluent®[13] was used. Given the assumed cylindrical and linear alignment of the simulated ITPTR systems, axi-symmetric, two-dimensional flow was assumed. Using a simple user defined function, the piston head motion was modeled as:

$$X = X_a * \sin(w*t) \tag{1}$$

where X_a= 4.511e-3 m, w = 213.62 r/s, and the time increment of 7.3529e-4 seconds were assumed.

Fluent is equipped with a dynamic meshing function that can create deformable mesh volumes. This function was utilized for modeling the compressor. Detailed nodalization of all components was performed, whereby regions deemed more sensitive, such as the vicinity of component-to-component junctions, were represented by finer mesh than others. The MOD1 and MOD2 systems were represented by a total of 4,325 and 4,366 nodes, respectively.

The mass, momentum and energy equations solved by Fluent for the forthcoming simulations are, respectively:

$$\frac{\partial \rho_f}{\partial t} + \frac{1}{r}\frac{\partial}{\partial r}(r \rho_f v_r) + \frac{\partial}{\partial x}(\rho_f v_x) = 0 \tag{2}$$

$$\frac{\partial}{\partial t}(\rho_f \vec{v}) + \nabla \cdot (\rho_f \vec{v}\vec{v}) = -\nabla p + \nabla \cdot (\tau) \tag{3}$$

$$\frac{\partial}{\partial t}(\rho_f E) + \nabla \cdot (\vec{v}(\rho_f E + p)) = \nabla \cdot \left(\hat{k}\nabla T + (\tau \cdot \vec{v})\right) \tag{4}$$

where

$$E = \hat{h} - \frac{p}{\rho} + \frac{v^2}{2} \tag{5}$$

and all properties represent the properties of the working fluid helium. The above equations apply to all components, except for CHX, WHX1, WHX2 and the regenerator. The latter 4 components are modeled as porous media, assuming that there is local thermodynamic equilibrium between the fluid and the solid structure in these components. The mass, momentum, and energy equations in the latter 4 components are:

$$\frac{\partial (\varepsilon \rho_f)}{\partial t} + \frac{1}{r}\frac{\partial}{\partial r}(\varepsilon r \rho_f v_r) + \frac{\partial}{\partial x}(\varepsilon \rho_f v_x) = 0 \tag{6}$$

$$\frac{\partial}{\partial t}(\varepsilon \rho_f \vec{v}) + \nabla \cdot (\varepsilon \rho_f \vec{v}\vec{v}) = -\varepsilon \nabla p + \nabla \cdot (\varepsilon \tau) - \left(\frac{\mu}{\beta}\vec{v} + \frac{1}{2}\hat{C}\rho_f |\vec{v}|\vec{v}\right) \tag{7}$$

$$\frac{\partial}{\partial t}\left(\varepsilon\rho_f E_f + (1-\varepsilon)\rho_s E_s\right) + \nabla\bullet\left(\vec{v}(\rho_f E_f + P)\right) = \nabla\bullet\left[\left(\varepsilon\hat{k}_f + (1-\varepsilon)\hat{k}_s\right)\nabla T + (\tau\bullet\vec{v})\right] \quad (8)$$

where $\varepsilon = 0.69$, $\beta = 1.06\times10^{-10}\,m^2$, and $\hat{C} = 7.609\times10^{4}\,m^{-1}$ were assumed. These parameters are based on the experiments of Harvey.[17]

For simplicity, all the simulations were done as transient processes, starting with an initial system temperature of 300 K for Cases 1-3, and 293 K for Cases 4-6. Simulations were continued until a steady-periodic state was obtained.

RESULTS AND DISCUSSION

General Observations

The variations of the cycle-average temperature of the CHX surface are depicted in Figure 2 for Cases 1, 2, 4 and 5, and show the development of steady-periodic states. For Cases 3 and 6, where a constant CHX surface temperature was imposed, steady periodic state can be easily recognized by plotting the temporal variation of the total rate of heat absorbed by the system through CHX (cooling load).

The axial distributions of cross-section and cycle-averaged temperature for Cases 1-3, under steady-periodic state, are displayed in Figure 3. Significant temperature gradients are predicted in the regenerator and the pulse tube. These profiles are evidently consistent with the known trends in data. The overall performances of the simulated systems are represented by the predicted entries in Table 2. Besides well-expected trends (e.g., higher cold tip temperatures with a cooling load of 1W, in comparison with cases with zero cooling load), an interesting observation is that simulation Cases 1-3 perform much better than Cases 4-6. The MOD1 system being made of models with large L/D, is evidently superior to the MOD2 system.

Multi-Dimensional Effects

Intuition suggests that multi-dimensional flow effects become more significant as a component's L/D ratio is reduced, and that the most significant multi-dimensional effects should occur at the vicinity of component-to-component junctions. Details of the simulation flow fields fully support these observations. Figures 4 and 5 depict the cycle-average temperature contours

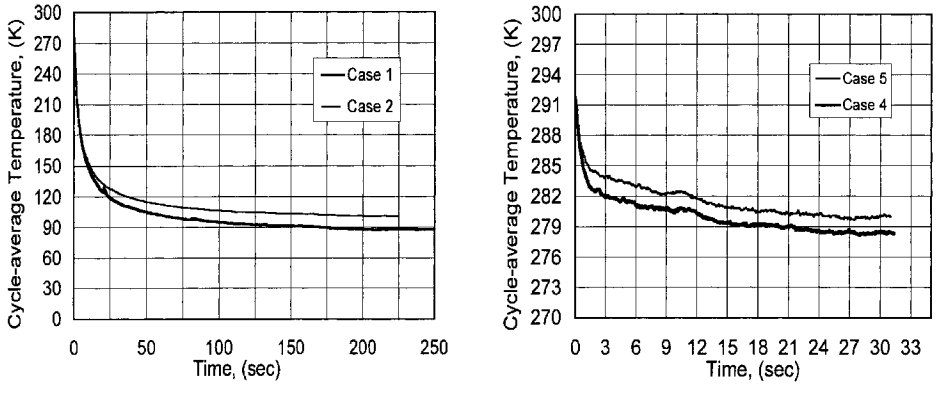

Figure 2. Temporal variations of cycle-average CHX surface temperature for simulation cases with a cooling load of 1W.

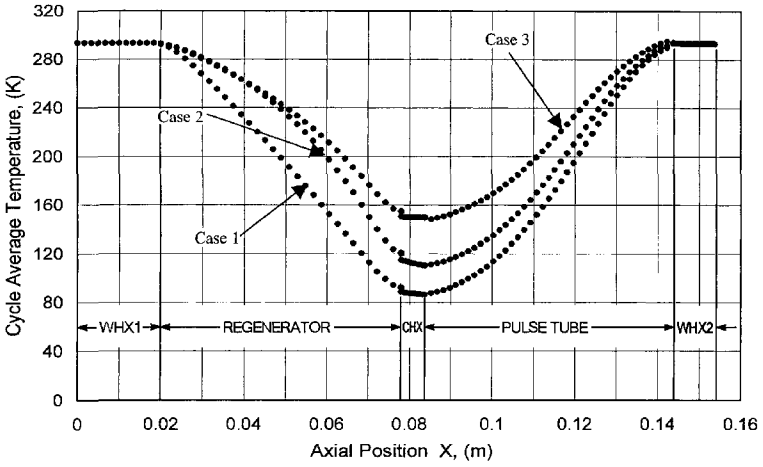

Figure 3. Axial distribution of cross-section and cycle-averaged temperature distributions under steady periodic for Cases 1-3 (MOD1 system).

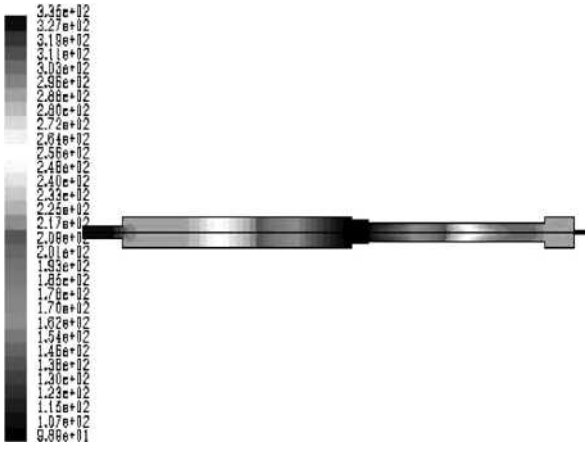

Figure 4. Steady-periodic cycle-average temperature contours for simulation Case 2.

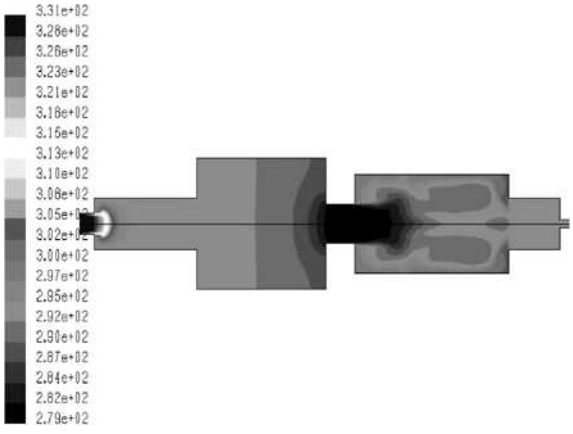

Figure 5. Steady-periodic cycle-average temperature contours for simulation Case 5.

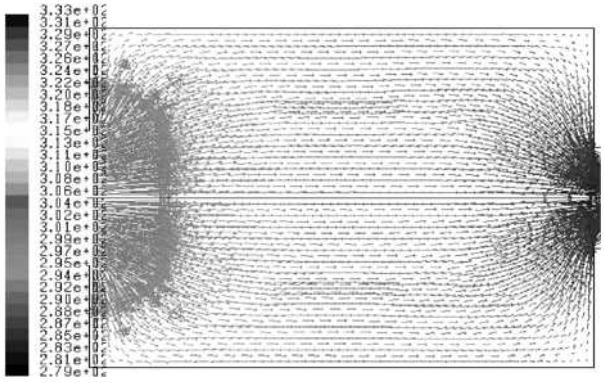

Figure 6. Snapshot of velocity vectors and temperatures [in K] in the regenerator of MOD2 system during the simulation Case 4.

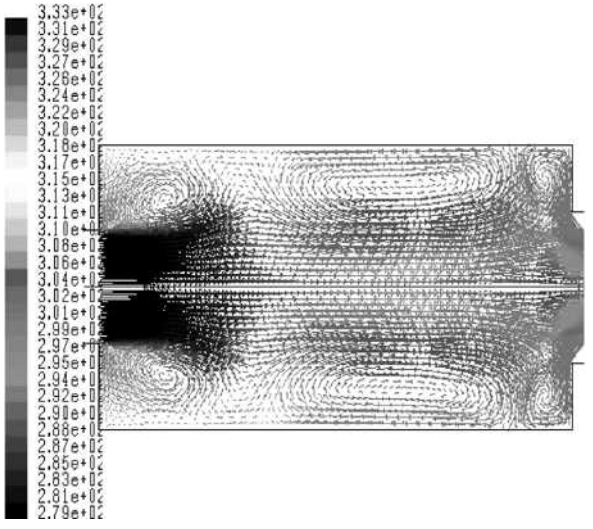

Figure 7. Snapshot of velocity vectors and temperatures [in K] in the pulse tube of MOD2 system during the simulation Case 4.

for Cases 2 and 5, respectively. The multi-dimensional effects in all simulations dealing with MOD1 system were relatively minor. Significant multi-dimensional effects occurred in MOD2 system, however. Typical snapshots of the fluid velocity and temperature distributions repre-senting the regenerator and the pulse tube of the MOD2 system are depicted in Figs. 6 and 7, respectively. The two figures are associated with Cases 4, under steady-periodic conditions. For both components, strong multi-dimensional effects occur near the two. The secondary flows, in the form of recirculation patterns are predicted for the pulse tube. The multi-dimensional flows undoubtedly impact pressure drop, dissipation and heat transfer processes, in particular in the regenerator. The multitude of recirculation pattern in the pulse tube cause undesirable mixing in the thermally stratified fluid, and is at least partially responsible for the poor overall performance of the MOD2 system.

CONCLUSION

Two entire ITPTR systems operating in steady periodic state under a variety of boundary conditions were numerically simulated using the CFD package Fluent. The objectives were to demonstrate the feasibility of CFD simulation of OPTRs, and to examine the multi-dimensional flow and

heat transfer effects. CFD simulations successfully predicted all the expected trends. They also showed that a 1-D analysis can be adequate only when all the components of the ITPTR have large length-to-diameter ratios. Significant multi-dimensional effects and working fluid recirculation occur when one or more components have relatively small L/D ratios. The recirculation patterns deteriorate the overall performance of the system.

ACKNOWLEDGEMENTS

The authors acknowledge gratefully the financial and technical support for this work by Raytheon Company.

NOTATION

$\hat{c}$ = Inertial Drag Coefficient
$\hat{h}$ = Enthalpy
$\hat{k}$ = Thermal Conductivity
P = Pressure
r = Radial coordinate
t = Time
T = Temperature
v = Velocity
w = Angular frequency (rad/s)
x = Axial coordinate
X = Piston displacement
X_a = Piston displacement amplitude

Greek letters

β = Permeability
ε = Porosity
μ = Absolute viscosity
ρ = Density
τ = Stress tensors

Subscripts

f = Fluid
s = Solid

REFERENCES

1. Gifford, W.E. and Longthworth, R.C., "Pulse-Tube Refrigeration," *Trans. ASME, J. Eng. Ind.* (series B), 86 (1964), pp. 264-268.
2. Mikulin, E.I., Tarasov, A.A., and Shrebyonock, M.P., "Low-temperature expansion pulse tubes," *Advances in Cryogenics Engineering*, vol 29, Plenum Publishing Corp., New York, pp. 629-637.
3. Zhu, S.W., Wu, P.Y., and Chen, Z.Q., " A single stage double inlet pulse tube refrigerator capable of reaching 42 K," ICEC 13 Proc. *Cryogenics*, 30 (1990), pp.256-261.
4. Wang, C., Wu, P., and Chen, Z., "Modified orifice pulse tube refrigerator without a reservoir," *Cryogenics*, 34 (1994), pp. 31-36.
5. Cai, J.H., Wang, J.J., Zhu, W.X. and Zhou, Y., "Experimental analysis of double-inlet principle in pulse tube refrigerator," *Cryogenics*, 33 (1993), pp. 522-525.
6. Zhu, S.W., Zhou, S.L., Yoshimura, N., and Matsubara, Y., "Phase shift effect of the long neck tube for the pulse tube refrigerator," *Cryocoolers 9*, Plenum Press, New York (1997), p. 269.
7. Ricardson, R.N. and Evans, B.E., "A review of pulse tube refrigeration," *Int. J. Refrigeration*, 20 (1997), pp. 367-373.
8. Popescu, G., Radcenco, V., Gargalian, E., and Bala, P.R., "A critical review of pulse tube cryogenerator research," *Int. J. Refrigeration*, 24 (2001), pp. 230-237.
9. Gedeon, D., *Pulse Tube Model-Class Reference Guide*, Gedeon Associates (1999).
10. Ju, Y.L., Wang, C. and Zhou, Y., "Numerical Simulation and Experimental Verification of the Oscillating Flow in Pulse Tube Refrigerator," *Cryogenics*, 38, pp. 160-176.
11. Hozumi, Y., Shiraishi, M., and Murakami, M., "Simulation of thermodynamics aspects about pulse tube refrigerator," *Adv. in Cryogenic Engineering*, Vol. 49B, Amer. Institute of Physics, Melville, NY (2004), pp. 1500-1507.
12. Flake, B. and Razani, A., "Modeling pulse tube cryocoolers with CFD," *Adv. in Cryogenic Engineering*, Vol. 49B, Amer. Institute of Physics, Melville, NY (2004), pp. 1493-1499.
13. Fluent Inc.,*Fluent 6 User Manual,* Fluent Inc (2003), p. 8-1.

14. Kirkconnell, C.S., *Numerical analysis of the mass flow and thermal behavior in high-frequency pulse tubes,* Ph.D. thesis, Georgia Institute of Technology, Atlanta (1995), GA.

15. Kirkconnell, C.S., Soloski, S.C., and Price, K.D., "Experiments on the Effects of Pulse Tube Geometry on PTR Performance," *Crycoolers 9*, Plenum Press, New York (1997), pp. 285.

16. Harvey, J.P., Kirkconnell, C.S., and Desai, P.V., "Comparison of Entropy Generation Rates in Various Stirling-Class Cryocooler Configurations," *Adv. in Cryogenic Engineering*, Vol. 49B, Amer. Institute of Physics, Melville, NY (2004), pp. 1519-1526.

17. Harvey, J.P., *Parametric study of cryocooler regenerator performance,* M.S. Thesis, Georgia Institute of Technology, Atlanta GA (1999).